Current on an Infinitely-Long Carbon Nanotube Antenna Excited by a Gap Generator

George W. Hanson, *Senior Member, IEEE*

***Abstract*—The current on an infinitely-long carbon nanotube (CN) antenna fed by a delta-gap source is studied using a Fourier transform technique. The CN is modeled as an infinitely-thin tube characterized by a semi-classical conductance, appropriate for the frequencies of interest considered in this work. The CN's current is compared with the current on solid and tubular copper antennas having similar or somewhat larger radius values. It is found that for radius values on the scale of nanometers, CNs exhibit smaller losses than cylindrical copper antennas having the same dimensions, assuming the bulk value of copper conductivity. When one assumes a more realistic, reduced copper conductivity that accounts for the nanoscopic radius of the wire, the advantage of the CN over a metallic wire is increased.**

***Index Terms*—Carbon nanotube (CN), cylindrical antennas, electromagnetic theory, nanotechnology.**

I. Introduction

A carbon nanotube (CN) is a cylinder made from a graphene sheet (i.e., a mono-atomic layer of graphite), typically having radius values of a few nanometers or less, and lengths (so far) up to centimeters [1]. Since their discovery in 1991 [2], CNs have been investigated for a wide array of applications. In the electronics area, CNs have been proposed as transistors [3], [4], transmission lines/interconnects [5], [6], nanotweezers [7], and field emission devices [8], among other uses. CNs can be either metallic or semiconducting, depending on their geometry, and either single walled (SWNT) or multiwalled (MWNT), although here we will focus on metallic SWNTs.

Since CNs can be grown having lengths on the order of centimeters, and can be metallic, a natural topic is to consider CNs for centimeter and millimeter wave antenna applications, as originally proposed in [9]. One application may be to provide a means to communicate with a nanoelectronic circuit. That is, as a means to connect the macroscopic "outside world" with a nanoscale circuit or device.

In a previous paper [10], it was found that a finite-length CN antenna exhibits impedance resonances when the tube length is approximately equal to integer values of $\lambda_p/2$, where λ_p is a plasma wavelength ranging from $0.015\lambda_0$ to $0.021\lambda_0$, with λ_0 being the free-space wavelength. However, this effect only occurs above the relaxation frequency; below the relaxation frequency resonances are strongly damped. Prior to [10], CN dipole antennas were considered based on a transmission-line model [9]. In this method, two parallel conductors form a transmission line, and the transmission line parameters inductance L, capacitance C, and resistance R, are determined for the line, based on the line geometry and materials. Then, the usual transmission line quantities, such as propagation constant, phase velocity, and characteristic impedance, are determined. The transmission line current due to an open-circuited end is obtained, and used to model the flared-out transmission line that forms a dipole antenna. The radiated field can then be obtained, and other antenna parameters determined from the approximate current distribution (which is a standing wave in the lossless case). Transmission line modeling of CNs is further considered in [6] and [11], and references therein.

The transmission line model illustrates several important characteristics of CN antennas. In particular, for a CN transmission line there exists a kinetic inductance L_K that dominates over the usual magnetic inductance [6]. Also, both the usual electrostatic capacitance, and a quantum capacitance, must be taken into account. One result is that the wave velocity on a CN transmission line is on the order of the Fermi velocity v_F, rather than the speed of light c (here we assume that the CN exists in free space). For a CN, $v_F \simeq 9.7 \times 10^5\ \mathrm{m/s}$, and the transmission line model predicts $v_p \simeq 0.01c$. As described later, here and in [10] it was found that the phase velocity is approximately $v_p \simeq 6.2 v_F \simeq 0.02c$, and is a moderately-weak function of frequency and geometry. Thus, wavelengths are much shorter on a CN, compared to on a macroscopic radius metallic tube. This is partly a purely geometric effect due to the small radius of the tube.

To investigate the basic properties of CN antennas it is worthwhile to consider an infinite antenna, removing the length-dependent current resonances, leaving only the tube's radius and the frequency of operation as parameters. The current induced on a gap-excited infinite antenna is considered here, where it is found that the antenna dynamics are primarily governed by the Sommerfeld pole. The CN is modeled using a semi-classical conductance derived explicitly for infinite CNs that is accurate through THz frequencies [12], [13]. At the frequencies of interest in this paper, this semi-classical conductivity is equivalent to the more rigorous (and complicated) quantum mechanical conductivity also derived in [12], [13], which accounts for interband transitions ignored in the semi-classical analysis.

II. Formulation

The CN is modeled as an infinitely-thin conducting tube having radius a and sheet conductance σ_{cn} (S). The tube is basically a cylinder formed by a graphene sheet. At an atomic level, graphene has the honeycomb structure shown in Fig. 1, where the small

Manuscript received February 19, 2005; revised August 28, 2005.

The author is with the Department of Electrical Engineering, University of Wisconsin-Milwaukee, Milwaukee, WI 53211 USA (e-mail: george@uwm.edu).

Digital Object Identifier 10.1109/TAP.2005.861550

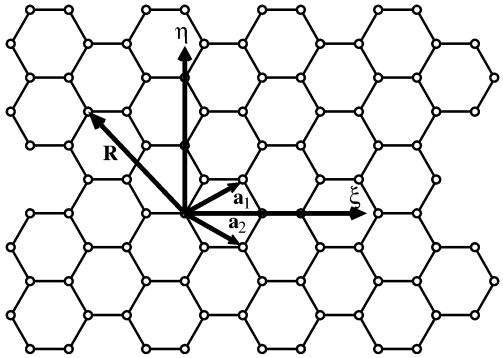

Fig. 1. Graphene sheet showing coordinate system, lattice basis vectors, and position vector. Circles denote the positions of carbon atoms.

circles denote the location of carbon atoms [14]. Lattice basis vectors are $\mathbf{a}_1$ and $\mathbf{a}_2$, as shown, and the relative position vector is $\mathbf{R} = m\mathbf{a}_1 + n\mathbf{a}_2$, where m, n are integers. A CN can be envisioned by wrapping the graphene sheet into a cylinder.

If the cylinder is formed around the ξ axis in Fig. 1, the resulting tube is called a zigzag CN. If the cylinder axis is the η axis in Fig. 1, the resulting tube is called an armchair CN, and if the cylinder axis is neither the ξ nor the η axis as shown, the resulting nanotube is called a chiral CN. Thus, CNs can be characterized by the dual index (m, n), where $(m, 0)$ for zigzag CNs, (m, m) for armchair CNs, and (m, n), $0 < n \neq m$, for chiral nanotubes. The resulting cross-section radius of a CN is given by [14]

$$a = \frac{\sqrt{3}}{2\pi} b \sqrt{m^2 + mn + n^2} \tag{1}$$

where $b = 0.142\ \mathrm{nm}$ is the interatomic distance in graphene.

CNs can be either metallic or semiconducting, depending on their geometry (i.e., on the values of m and n) [14], [15]. Armchair CNs are always metallic (i.e., they exhibit no energy bandgap), as are zigzag CNs with $m = 3q$, where q is an integer. In this work metallic (armchair) CNs will be exclusively considered.

Assuming that the axis of the CN is the z-axis, the current on the tube can be written as

$$\mathbf{J}(\mathbf{r}) = \hat{\mathbf{z}} J_z(z)\, \delta(\rho - a) \tag{2}$$

such that the axial current flowing on the tube is

$$\begin{aligned} I(z) &= \int_0^a \int_0^{2\pi} J_z(z)\, \delta(\rho - a)\, \rho d\phi d\rho \\ &= J_z(z)\, 2\pi a. \end{aligned} \tag{3}$$

The semi-classical CN conductance is derived starting with Boltzmann's equation specialized to the case of a z-directed, ϕ-independent electric field E_z, with the resulting current flowing solely in the z-direction under the relaxation-time approximation. For small radius metallic CNs, σ_{cn} (S) can be approximated by [12], [13]

$$\sigma_{cn}(\omega) \simeq -j \frac{2e^2 v_F}{\pi^2 \hbar a (\omega - j\nu)} \tag{4}$$

where $v_F \simeq 9.7 \times 10^5\ \mathrm{m/s}$ is the Fermi velocity for a CN, $-e$ is the electron's charge, ν is the relaxation frequency ($\nu = \tau^{-1}$, where τ is the relaxation time), and $\hbar$ is the reduced Planck's constant. The integral equation for surface current density (A/m) can be obtained from Ohm's law

$$J_z(z, \omega) = \sigma_{cn}(\omega)\, E_z(z, \omega) \tag{5}$$

for all z along the tube. Expressing the electric field as the sum of an impressed field and the field due to the resulting current leads to the standard Pocklington integral equation [16], [17]

$$\begin{aligned} \left(k^2 + \frac{\partial^2}{\partial z^2}\right) \int_{-\infty}^{\infty} K(z - z')\, I(z') dz' \\ = j4\pi\omega\varepsilon z_{cn} I(z) - j4\pi\omega\varepsilon E_z^i(z) \end{aligned} \tag{6}$$

where

$$z_{cn} = \frac{1}{2\pi a \sigma_{cn}} \tag{7}$$

is an impedance per unit length, $K(z - z')$ is the exact (for an infinitely-thin tube) kernel

$$K(z - z') = \frac{1}{2\pi} \int_{-\pi}^{\pi} \frac{e^{-jk\sqrt{(z-z')^2 + 4a^2 \sin^2(\phi'/2)}}}{\sqrt{(z - z')^2 + 4a^2 \sin^2(\phi'/2)}} d\phi' \tag{8}$$

and E_z^i is the impressed excitation, here assumed to be a gap generator. Equation (6) is the same IE that would be obtained for an infinitely-thin metallic tube if σ_{cn} is replaced by the sheet conductance of the tube. However, in contradistinction to the case of a metal tube, end effects at the CN's gap excitation will alter the energy band structure near the tube ends, changing the local conductance. However, for a long nanotube antenna this effect can be expected to be small, and is ignored here.

Using Fourier transform methods [17]–[19], (6) can be solved as

$$I(z) = j4\pi\omega\varepsilon \int_{-\infty - j\delta}^{\infty + j\delta} \frac{f(\alpha)\, e^{-j\alpha z}}{Z(\alpha)} d\alpha \tag{9}$$

where $\delta > 0$ is a small parameter

$$\begin{aligned} Z(\alpha) = 2\left(\alpha^2 - k^2\right) I_0\left(a\sqrt{\alpha^2 - k^2}\right) K_0\left(a\sqrt{\alpha^2 - k^2}\right) \\ + j4\pi\omega\varepsilon z_{cn} \end{aligned} \tag{10}$$

and

$$E_z^i(z) = \int_{-\infty}^{\infty} f(\alpha)\, e^{-j\alpha z} d\alpha \tag{11}$$

and where I_0 and K_0 are modified Bessel functions [20]. The factor $Z(\alpha)$ is multivalued in the α-plane due to the Bessel function K_0, and branch points appear at $\alpha = \pm k$. Branch cuts are chosen along the real-α axis, and exist along $-\infty < \alpha \leq -k$, and $k \leq \alpha < \infty$. The path of integration in (9) is parallel to, and just below, the real axis for $-\infty < \alpha \leq 0$, and parallel to, and just above, the real axis for $0 \leq \alpha < \infty$, as shown in [19, p. 499].

As a special case, for a delta-gap source

$$E_z^i(z) = V_0 \delta(z) \tag{12}$$

(so that $f(\alpha) = V_0/2\pi$), and replacing z by $|z|$ we obtain

$$I(z) = \frac{j4\pi\omega\varepsilon V_0}{2\pi} \int_{-\infty - j\delta}^{\infty + j\delta} \frac{e^{-j\alpha|z|}}{Z(\alpha)} d\alpha. \tag{13}$$

The integral (6) and resulting solution (13) is identical to the case of a thin-walled (with respect to the free-space wavelength), imperfectly conducting tubular metallic wire antenna [21], if one substitutes z_m for z_{cn}, where z_m is the metal antenna's impedance per unit length. For metal tubular antennas, if the wall thickness d is much greater than the skin depth $\delta_s = (2/\omega\mu\sigma_{3d})^{1/2}$[21]

$$z_m = \frac{1+j}{2\pi a\sigma_{3d}\delta_s} \tag{14}$$

and if d is thin compared to the skin depth

$$z_m = \frac{1}{2\pi a\sigma_{3d}d} \tag{15}$$

where σ_{3d} is the usual conductivity of the metal (S/m)

$$\sigma_{3d}(\omega) = -j\frac{e^2N_e^{3d}}{m_e(\omega - j\nu)}. \tag{16}$$

In (16), N_e^{3d} is the three-dimensional electron density and m_e is the electron's mass. Therefore, we can see that the conductance (4), σ_{cn}, plays the same role as the product of bulk conductivity and wall thickness (i.e., $\sigma_{3d}d$) for a thin yet finite-thickness metal tube. The same integral equation and solution also holds for a solid cylindrical conductor if one uses the impedance [21]

$$z_m = \frac{\gamma J_0(\gamma a)}{2\pi a\sigma_{3d}J_1(\gamma a)} \tag{17}$$

where

$$\gamma = (1-j)\sqrt{\frac{\omega\mu\sigma_{3d}}{2}} \tag{18}$$

and where J_0 and J_1 are the usual first-kind Bessel functions.

Following the method detailed in [19, pp. 451–453] for metallic antennas, the integral (13) can be written as a branch cut integral and a sum of residues

$$I(z) = \sum_n I_n(z) + I_{bc}(z) \tag{19}$$

where

$$I_n(z) = -2\pi jR_n^{\text{res}}(z) = 4\pi\omega\varepsilon V_0\frac{e^{-j\alpha_n|z|}}{Z'(\alpha_n)} \tag{20}$$

with $Z' = \partial Z/\partial\alpha$, and where the roots α_n satisfy $Z(\alpha_n) = 0$. The branch cut integral can be written as

$$I_{bc}(z) = \frac{2\omega\varepsilon kV_0}{j\pi}\int_0^\infty du\frac{u}{\sqrt{u^2-1}} \times\left\{\frac{e^{-k\sqrt{u^2-1}|z|}}{-k^2u^2J_0(aku)H_0^{(1)}(aku)+4\omega\varepsilon z_{cn}} - \frac{e^{-k\sqrt{u^2-1}|z|}}{k^2u^2J_0(aku)H_0^{(2)}(aku)+4\omega\varepsilon z_{cn}}\right\} \tag{21}$$

where $H_0^{(1,2)}$ are the usual Hankel functions. The branch cut integral has much better convergence properties than the original integral (13), and is used for computing results in this work.

As described in [22], although there is more than one pole for an imperfectly conducting metal wire, only the principle pole (sometimes called the Sommerfeld pole) is not severely damped. This is also found to be the case for metallic CNs, and, denoting this pole by $\beta = \alpha_0$, (19) reduces to

$$I(z) = I_{\text{res}}(z) + I_{bc}(z) \tag{22}$$

where $I_{\text{res}}(z) = 4\pi\omega\varepsilon V_0e^{-j\beta|z|}/Z'(\beta)$.

TABLE I
COMPARISON OF THE RESULTS (22) AND ADMITTANCE VALUES IN [23, FIG. 1] (WHICH USES A MAGNETIC-FRILL SOURCE), FOR VALIDATION OF THE SOLUTION (22), SHOWING THE COMPLEX CURRENT IN μA AT $z = 2\lambda = 2$ m ON AN INFINITE-LENGTH CYLINDRICAL METALLIC DIPOLE ANTENNA; $F = 300$ MHz, $a = 0.01$ cm, AND $V_0 = 1$ V

δ_s/a	I_{res}	I_{bc}	$I = I_{bc} - I_{res}$	$I_{[24]}$
1	$-472.8, 85.1$	$-49.9, 18.0$	$422.8, -67.1$	419
2	$-753.4, 144.9$	$-15.58, 69.6$	$737.8, -75.2$	740
4	$-832.1, 107.8$	$17.40, 90.1$	$849.5, -17.6$	840

The solution (22) was verified in several ways. First, it was checked numerically that (22) yielded the same result as the original integral (13). Furthermore, although it would be useful to directly compare results with other simulations or measurements for $I(z)$ on a CN, no such results seem to be available in the literature. However, note that the principle difference between the integral equation for a CN dipole, and that for an ordinary metallic dipole, is the value of impedance used, either (7) for the CN, or one of (14), (15), or (17) for a metal dipole. Therefore, using (17), a comparison was made between (22) and the results in [23], which concerns a solid cylindrical infinite-length metallic antenna having finite conductivity. In that paper, a magnetic-frill source was used. However, sufficiently far from the source the current due to a magnetic-frill and a delta gap should be the same [18, p. 294]. The largest distance available for comparison in [23] is $z/\lambda = 2$, which is large enough so that the results should be at least fairly comparable. As shown in Table I, (22) agrees relatively well with the results in [23], considering that the excitations are different.

As a further check, if one considers a finite-length gap-excited CN dipole that is sufficiently long, so that all energy is dissipated before the current reaches the end of the antenna, then the current on a finite CN dipole, and that on an infinite CN antenna, should agree. In [10] the integral equation analogous to (6) for a finite-length CN dipole antenna was converted to Hallén form, and solved via the method of moments (MoM). That pulse-function, point matching solution, when applied to the case of an ordinary metallic dipole antenna, was itself verified by comparison to the results for imperfectly conducting finite-length metallic dipoles [21], [24], and [25]. The MoM solution of [10] for a finite, relatively long (800 μm) CN antenna was then compared to the Fourier transform result (22), and the results are shown in Fig. 2, where the difference in the two solutions is virtually indistinguishable on the scale of the plot. Therefore, we conclude that the solution (22) is accurate. In the results presented here, the relaxation frequency for the CN is taken as $\nu = \left(3\times10^{-12}\right)^{-1}$, $f = \nu/2\pi \simeq 53$ GHz [13], although in the literature a range of values $O\left(10^{-12}\right) - O\left(10^{-13}\right)$ have been measured.

Finally, it should be noted that in [12] and [13], rather than (5), the relation between current density and electric field is

$$\left(1+\xi\frac{\partial^2}{\partial z^2}\right)J_z(z,\omega) = \sigma_{cn}(\omega)E_z(z,\omega) \tag{23}$$

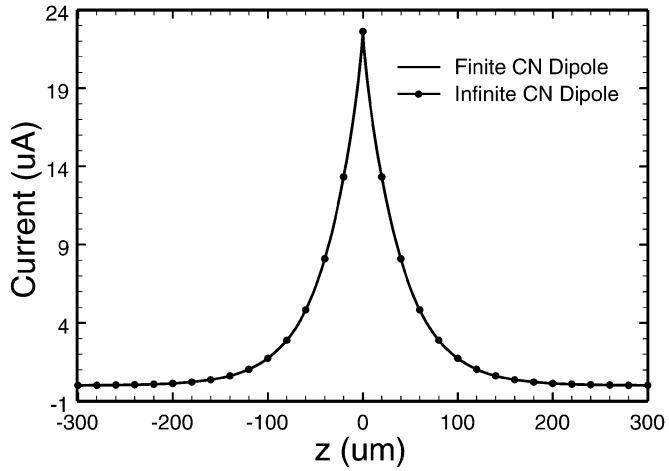

Fig. 2. Comparison of (22) with results from a MoM solution for a finite CN dipole [10] having total length 800 μm, $a = 2.712$ nm, $F = 100$ GHz, and $V_0 = 1$ V.

where

$$\xi = \frac{L_0}{k^2\left(1 - \frac{j\nu}{\omega}\right)^2} \tag{24}$$

with $L_0 \simeq 10^{-5}$. This modified form of Ohm's law results from assuming a travelling wave with slow variation for the electric field and current when solving Boltzmann's equation. For a finite-length antenna this assumption may not be appropriate since fields and currents may not exhibit travelling wave behavior, and so in [10] the term involving ξ, which is relatively small compared to unity, was ignored. Ignoring this term is equivalent to assuming that fields and currents are constant over length scales associated with electron collisions (the mean-free path), which is the usual assumption in solving Boltzmann's equation for macroscopic conductors.

For an infinite CN antenna one expects travelling wave behavior, and, therefore, inclusion of this term may be appropriate. The integral equation resulting from (23) is

$$\left(k^2 + \frac{\partial^2}{\partial z^2}\right)\int_{-\infty}^{\infty} K\left(z - z'\right) I(z')dz' = j4\pi\omega\varepsilon z_{cn}\left(1 + \xi\frac{\partial^2}{\partial z^2}\right) I(z) - j4\pi\omega\varepsilon E_z^i(z) \tag{25}$$

and the solution of (25) merely differs from the solution of (6) by substituting

$$z_{cn}(\alpha) = z_{cn}\left(1 - \xi\alpha^2\right) \tag{26}$$

in place of z_{cn} in (10) and (21).

In Fig. 3 a comparison is shown for the principle pole β of an $a = 2.712$ nm CN, computed from (10) with and without the $\xi\alpha^2$ term. The velocity factor s_r, is the phase velocity normalized by the speed of light, i.e., $s_r = v_p/c$, where $v_p = \omega/Re(\beta)$, such that small s_r indicates slower velocity. It can be seen that the term $\xi\alpha^2$ has a negligible effect on the results [also verified for the current density obtained from (22)], and so this term will be omitted in the following.

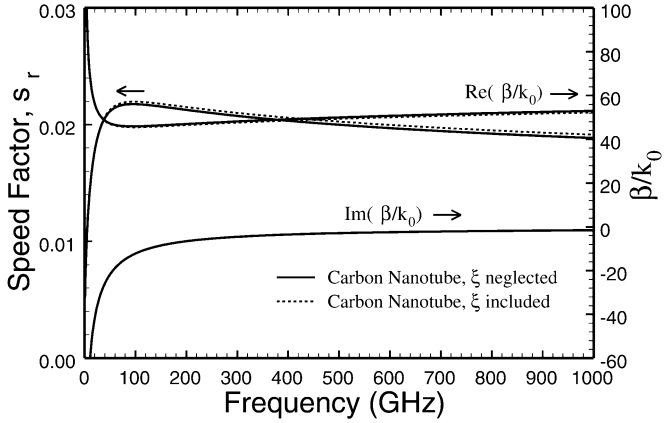

Fig. 3. Comparison for the principle pole β of an $a = 2.712$ nm CN, computed from (10) with and without the $\xi\alpha^2$ term in (26).

TABLE II
CURRENT (μA) ON AN INFINITE CARBON NANOTUBE DIPOLE DUE TO THE RESIDUE AND THE BRANCH CUT CONTRIBUTIONS, AND THE TOTAL CURRENT; $a = 2.712$, $F = 100$ GHz

z (μm)	I_{res}	I_{bc}	$I = I_{bc} - I_{res}$
2	$-21.26, -0.72$	$-0.39, 1.19$	$20.88, 2.05$
20	$1.71, 13.33$	$-0.082, 0.116$	$-1.80, -13.21$
200	$-0.133, 0.023$	$-0.00049, 0.00037$	$-0.133, 0.023$

III. RESULTS

We first consider an infinite CN having radius $a = 2.712$ nm [corresponding to $m = n = 40$ in (1)], excited by a $V_0 = 1$ volt gap generator at $z = 0$ (in all results we assume the position of the source to be at the origin, and that $V_0 = 1$ V). The current at three different positions along the antenna is shown in Table II, for $F = 100$ GHz, where the total current is given, as well as the contributions to the current due to the residue and branch cut. It can be seen that the residue provides the dominant contribution to the current, at least at the frequency considered. This is also true for ordinary metallic cylinders. Moreover, for the CN this was also found to be true at other frequencies in the 1–1000 GHz range.

Fig. 4 shows the normalized principle pole β/k_0, versus frequency for CNs having different radius values spanning a typical range ($a = 2.712$, 1.356, and 0.678 nm), and for several solid and tubular cylindrical copper antennas. For the tubular conductors, the thickness of the tube was held constant at 10 nm, and the outer radius of the tube was varied. The two unlabeled curves in Fig. 4(a), between the 10 nm and 100 nm solid cylinder results, are for a tubular wire having outer radius values 20 nm for the upper curve, and 60 nm for the lower curve. In Fig. 4(b), these tube results are labeled as a/d, where a is the outer radius and d is the tube wall thickness.

Before discussing the results in Fig. 4, it should be noted that in order to make a comparison between CN antennas and metallic antennas, we obviously need to know the conductivity σ_{3d} for nanoscopic radius metal cylinders. For ordinary metals such as copper, the formula (16) should hold down to wire radius values on the order of 80 nm. As a rough approximation, the conductivity (16) should hold for metals much larger (in all directions) than the mean-free path length, which is approximately 40 nm for copper at room temperature (i.e., there should be many electron collisions for the semi-classical result (16) to be valid).

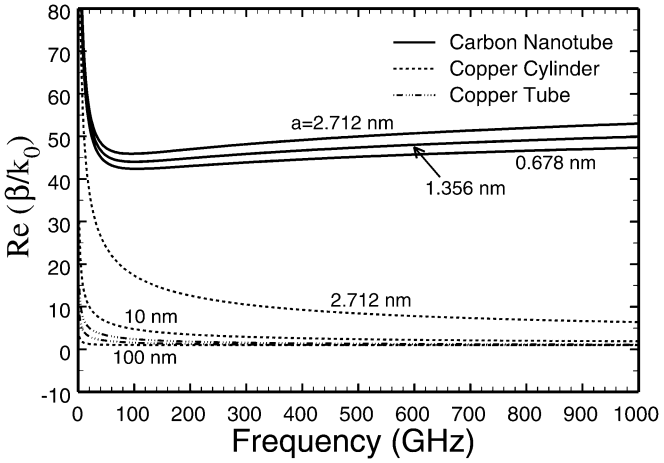

(a)

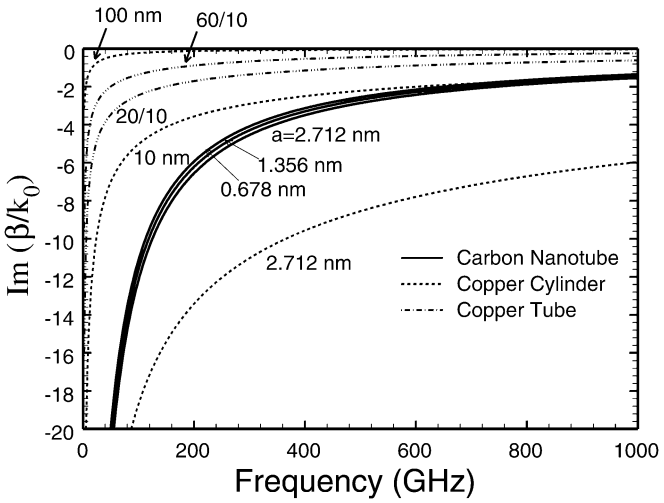

(b)

Fig. 4. (a) Real part of normalized propagation constant versus frequency for the principle pole of CN antennas, copper cylinder (solid) antennas, and tubular copper antennas. The two (unlabeled) curves between the 10 nm and 100 nm solid cylinder results are for a tubular wire having wall thickness 10 nm, and radius values 20 nm for the upper curve, and 60 nm for the lower curve. (b) Imaginary part of normalized propagation constant versus frequency for the principle pole of CN antennas, copper cylinder (solid) antennas, and tubular copper antennas.

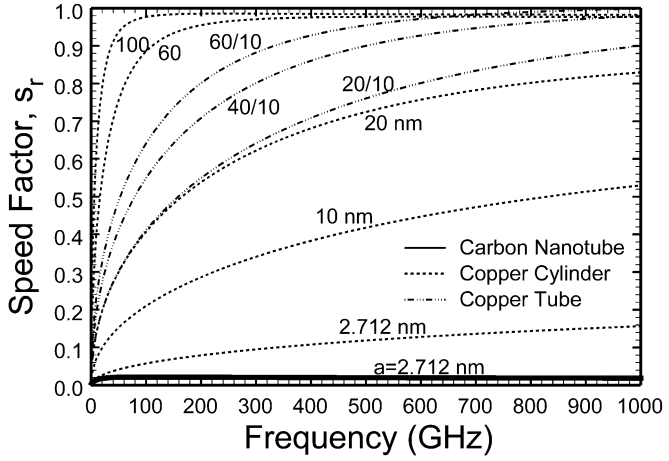

Fig. 5. Speed factor s_r for a CN antenna, and for various copper cylinder (solid) and tubular antennas. For the tubular antennas, results are labeled as a/d, where a is the outer radius and d is the wall thickness.

However, at this time the value of conductivity for metal cylinders having radius values on the order of a mean free path, or less, is somewhat unknown. For example, recent measurements on rectangular cross-section copper traces indicate that when lateral dimensions fall below 100 nm, surface and grain boundary scattering cause a significant increase in resistivity. In particular, for 50 nm $\times$ 50 nm copper traces considered in [27], the measured resistivity was approximately twice as large as the bulk value for copper. Furthermore, resistivity was shown to increase sharply as dimensions were reduced, although in that paper no values were presented under 40 nm (although it can be inferred that resistivity may increase by several orders of magnitude as the cross-sectional dimension is further reduced to the 1–10 nm range). In addition, impurities and material imperfections will also exert a strong influence in extremely small dimension metallic traces, in contrast to the case of a CN, which can be grown practically without defects. In this paper, to provide a contrast to the CN results, and to avoid somewhat arbitrarily choosing a value of conductivity, the bulk conductivity of copper will be used (i.e., (16), where $\nu \simeq \left(2.47 \times 10^{-14}\right)^{-1}$ and $N_e^{3d} \simeq 8.45 \times 10^{28}$ electrons/m^3 [28], leading to, for example, $\sigma_{3d} \simeq 5.88 \times 10^7 - j9.13 \times 10^4$ S/m at 10 GHz). This will be referred to as bulk approximated copper in the following. However, it should be recognized that the resulting conductivity may be far too large. Furthermore, for radius values on the order of several nanometers, quantum confinement effects in the radial coordinate begin to play a role, since these lengths begin to become comparable to the electron's de Broglie wavelength, λ_e, which is approximately 0.5 nm, although this effect won't be included here.

From Fig. 4 it can be seen that the real part of the propagation constant for a CN is much larger than for similarly-sized solid and tubular metallic (bulk-approximated) conductors, and therefore the wave is slower on a CN antenna. As radius increases for the metal antennas, the real part of β approaches k_0, as is the usual case on a macroscopic thin-wire antenna. Because of the relatively larger value of β on the CN antenna, the velocity factor $s_r = v_p/c = \omega/c\,\mathrm{Re}\,(\beta)$ is smaller on the CN antenna than for the metallic antenna. This is shown in Fig. 5, for an $a = 2.712$ nm CN antenna, and for various (bulk-approximated) solid and tubular cylindrical metal wires (where again, for the tubular metallic antennas, results are labeled as a/d, where a is the outer radius and d is the wall thickness). For the CN, only the $a = 2.712$ nm result is shown, since the results are only weakly dependent of CN radius, assuming reasonable radius ($a = 0.5$–3 nm) tubes. Fig. 3 also shows the CN result on a smaller scale, where it can be seen that the phase velocity is a relatively weak function of frequency in the range shown.

Losses on the antenna are indicated by the imaginary part of β. As can be seen in Fig. 4(b), losses on nanometer radius tubes (both copper cylinders and CNs) can be quite high, due to the extremely small radius values. However, CNs are relatively better conductors than (bulk-approximated) copper, as can be seen by comparing the CN result with the result for a solid cylinder having the same radius ($a = 2.712$ nm; note again that at this extremely small radius the copper's conductivity would actually be much lower that the bulk value assumed here, increasing losses even further). Despite the fact that the metal cylinder is solid, and that the CN is modeled as an infinitely-thin tube, the

CN has a smaller value of $\mathrm{Im}\,(\beta/k_0)$, thus signifying lower loss. At, for instance, $F = 500$ GHz, $\alpha_{cn}/k_0 = -\mathrm{Im}\,(\beta_{cn}/k_0) \simeq 2.8$ for the CN, and $\alpha_m/k_0 = -\mathrm{Im}\,(\beta_m/k_0) \simeq 8.4$ for a metal cylinder. Thus, the standard formula for power attenuation

$$A_p = 8.686\,\alpha_{cn/m}\ \mathrm{dB\ m^{-1}} \tag{27}$$

results in $A_p = 0.255\ \mathrm{dB}/\mu\mathrm{m}$ for the CN, and $A_p = 0.765\ \mathrm{dB}/\mu\mathrm{m}$ for the solid copper wire, where for both cases $a = 2.712\,\mathrm{nm}$. The CN antenna suffers roughly three times less power attenuation than the solid copper cylinder at this radius, even assuming the bulk value of conductivity for copper. As mentioned previously, the "wildcard" is, to some extent, the value of the metal's conductivity. At small size scales, surface roughness, impurities, and other fabrication aspects would play a key role in determining the correct value of metal conductivity. It would be expected that these aspects would, in many cases, further lower, perhaps drastically, the metal's conductivity (compared to the bulk value), making CNs even more advantageous. For example, assuming a solid copper cylinder having $a = 2.712\,\mathrm{nm}$, and decreasing the conductivity by a factor of ten from the bulk value, then $\mathrm{Re}\,(\beta/k_0) = 28.57$ and $\mathrm{Im}\,(\beta/k_0) = -29.70$ at $F = 500$ GHz. In this case, $A_p = 2.702\,\mathrm{dB/m}$, which is ten times worse that the CN result. Of course, attenuation can be greatly reduced by using larger radius metal cylinders, say, $a \sim O\,(100\,\mathrm{nm})$ or more. However, to attach to nanoscopic circuits one may need to use interconnects or antennas with radius values on the order of several nanometers, and at this scale CNs seem to be superior to metallic tubes or cylinders.

IV. Conclusion

The current on an infinite CN antenna fed by a delta-gap source has been studied, and its characteristics compared with solid and tubular copper antennas having nanometer-scale radius values. The CN is modeled as an infinity-thin tube characterized by a semi-classical conductivity. It is found that for radius values on the scale of nanometers, CNs exhibit significantly less loss than cylindrical copper antennas having the same dimensions. Thus, if radius values on the order of a nanometer are necessary, for instance, as part of a nanoelectronic circuit, CNs may be an appropriate choice as an antenna or interconnect.

References

[1] S. Li, Z. Yu, C. Rutherglan, and P. J. Burke, "Electrical properties of 0.4 cm long single-walled CNs," *Nano Lett.*, vol. 4, pp. 2003–2007, 2004.

[2] I. Iijima, "Helical microtubules of graphitic carbon," *Nature*, vol. 354, pp. 56–58, 1991.

[3] S. Li, Z. Yu, S. F. Yen, W. C. Tang, and P. J. Burke, "Carbon nanotube transistor operation at 2.6 GHz," *Nano Lett.*, vol. 4, pp. 753–756, 2004.

[4] J. P. Clifford, D. L. John, L. C. Castro, and D. L. Pulfrey, "Electrostatics of partially gated carbon nanotube FETs," *IEEE Trans. Nanotechnol.*, vol. 3, pp. 281–286, Jun. 2004.

[5] P. J. Burke, "Lüttinger liquid theory as a model of the GHz electrical properties of CNs," *IEEE Trans. Nanotechnol.*, vol. 1, pp. 129–144, Sep. 2002.

[6] ——, "An RF circuit model for CNs," *IEEE Trans. Nanotechnol.*, vol. 2, pp. 55–58, Mar. 2003.

[7] P. Kim and C. M. Lieber, "Nanotube nanotweezers," *Science*, vol. 286, pp. 2148–2150, 1999.

[8] G. Pirio, P. Legagneux, D. Pribat, K. B. K. Teo, M. Chhowalla, G. A. J. Amaratunga, and W. I. Milne, "Fabrication and electrical characteristics of carbon nanotube field emission microcathodes with an integrated gate electrode," *Nanotechnol.*, vol. 13, pp. 1–4, Feb. 2002.

[9] P. J. Burke, S. Li, and Z. Yu, "Quantitative theory of nanowire and nanotube antenna performance," IEEE Trans. Nanotechnol., 2005, submitted for publication.

[10] G. W. Hanson, "Fundamental transmitting properties of carbon nanotube antennas," *IEEE Trans. Antennas Propag.*, vol. 53, no. 11, pp. 3426–3435, Nov. 2005.

[11] J. J. Wesström, "Signal propagation in electron waveguides: Transmission-line analogies," *Phys. Rev. B*, pp. 11 484–11 491, Oct. 1996.

[12] S. A. Maksimenko, G. Y. Slepyan, A. Lakhtakia, O. Yevtushenko, and A. V. Gusakov, "Electrodynamics of CNs: Dynamic conductivity, impedance boundary conditions, and surface wave propagation," *Phys. Rev. B*, vol. 60, pp. 17 136–17149, Dec. 1999.

[13] S. A. Maksimenko and G. Y. Slepyan, "Electrodynamic properties of CNs," in *Electromagnetic Fields in Unconventional Materials and Structures*, O. N. Singh and A. Lakhtakia, Eds. New York: Wiley, 2000.

[14] R. Saito, G. Dresselhaus, and M. S. Dresselhaus, *Physical Properties of Carbon Nanotubes*. London, U.K.: Imperial College Press, 2003.

[15] Z. Yao, C. Dekker, and P. Avouris, "Electrical transport through single-wall CNs," in *Carbon Nanotubes; Topics in Applied Physics*, M. S. Dresselhaus, G. Dresselhaus, and P. Avouris, Eds. Berlin: Springer Verlag, 2001, vol. 80, pp. 147–171.

[16] R. S. Elliott, *Antenna Theory and Design*. Englewood Cliffs, NJ: Prentice-Hall, 1981.

[17] T. T. Wu, "Introduction to linear antennas," in *Antenna Theory*, R. E. Collin and F. J. Zucker, Eds. New York: McGraw-Hill, 1969, pt. 1, ch. 8.

[18] D. S. Jones, *Methods in Electromagnetic Wave Propagation*, New York: IEEE Press, 1994.

[19] E. Hallén, *Electromagnetic Theory*. New York: Wiley, 1962.

[20] M. Abramowitz and I. A. Stegun, Eds., *Handbook of Mathematical Functions with Formulas, Graphs, and Mathematical Tables*, 9th ed. New York: Dover, 1972.

[21] R. W. P. King and T. T. Wu, "The imperfectly conducting cylindrical transmitting antenna," *IEEE Trans. Antennas Propag.*, vol. AP-14, no. 5, pp. 524–534, Sep. 1966.

[22] J. A. Stratton, *Electromagnetic Theory*. New York: McGraw-Hill, 1941.

[23] J. H. Richmond, "Admittance of infinitely long cylindrical wire with finite conductivity and magnetic frill excitation," *IEEE Trans. Antennas Propag.*, vol. AP-27, no. 2, pp. 264–266, Mar. 1979.

[24] C. D. Taylor, C. W. Harrison, and E. A. Aronson, "Resistive receiving and scattering antenna," *IEEE Trans. Antennas Propag.*, vol. AP-15, no. 3, pp. 371–376, May 1967.

[25] B. D. Popović and Z. D. Popović, "Imperfectly conducting cylindrical antenna: variational approach," *IEEE Trans. Antennas Propag.*, vol. AP-19, no. 3, pp. 435–536, May 1971.

[26] N. Trivedi and N. W. Ashcroft, "Quantum size effects in transport properties of metallic films," *Phys. Rev. B*, vol. 38, pp. 12 298–12 309, Dec. 1988.

[27] W. Steinhögl, G. Schindler, G. Steinlesberger, M. Traving, and M. Engelhardt, "Comprehensive study of the resistivity of copper wires with lateral dimensions of 100 nm and smaller," *J. Appl. Phys.*, vol. 97, pp. 023 706-1–7, 2005.

[28] C. Kittel, *Introduction to Solid State Physics*, 6th ed. New York: Wiley, 1986.

George W. Hanson (S'85–M'91–SM'98) was born in Glen Ridge, NJ, in 1963. He received the B.S.E.E. degree from Lehigh University, Bethlehem, PA, the M.S.E.E. degree from Southern Methodist University, Dallas, TX, and the Ph.D. degree from Michigan State University, East Lansing, in 1986, 1988, and 1991, respectively.

From 1986 to 1988 he was a Development Engineer with General Dynamics in Fort Worth, TX, where he worked on radar simulators. From 1988 to 1991, he was a research and teaching assistant in the Department of Electrical Engineering at Michigan State University. He is currently Associate Professor of Electrical Engineering and Computer Science at the University of Wisconsin in Milwaukee. His research interests include electromagnetic analysis of nanostructures, electromagnetic wave phenomena in layered media, integrated transmission lines, waveguides and antennas, leaky waves, and mathematical methods in electromagnetics.

Dr. Hanson is a member of the International Union of Radio Science (URSI) Commission B, Sigma Xi, and Eta Kappa Nu. He is an Associate Editor for the IEEE Transactions on Antennas and Propagation.